Nano World Journal

http://dx.doi.org/10.17756/nwj.2015-004

Research Article

Open Access

Nanoprobe NAPPA Arrays for the Nanoconductimetric Analysis of Ultra-Low-Volume Protein Samples Using Piezoelectric Liquid Dispensing Technology

Eugenia Pechkova[1*], Wiktor Peter[2], Nicola Bragazzi[3], Festa Fernanda[2] and Claudio Nicolini[1,2,3]

[1]Laboratories of Biophysics and Nanobiotechnology (LBN), Department of Experimental Medicine (DIMES), University of Genoa, Via Pastore 3, 16132, Genova, Italy
[2]Virginia G. Piper Center for Personalized Diagnostics, Biodesign Institute, Arizona State University (ASU), Tempe, Arizona 85287, USA
[3]Nanoworld Institute, Fondazione EL.B.A. Nicolini (FEN), Largo Redaelli 7, 24020, Pradalunga, Bergamo, Italy

[*]Correspondence to:
Prof. Eugenia Pechkova, PhD
Laboratories of Biophysics and Nanobiotechnology
Department of Experimental Medicine
University of Genova Medical Schoool
Via Pastore, 3, 16132 Genova, Italy
Tel: +39-010-353-38217
Fax: +39-010-353-38215
E-mail: epechkova@ibf.unige.it

Received: February 18, 2015
Accepted: March 17, 2015
Published: March 19, 2015

Citation: Pechkova E, Peter W, Bragazzi N, Fernanda F, Nicolini C. 2015. Nanoprobe NAPPA Arrays for the Nanoconductimetric Analysis of Ultra-Low-Volume Protein Samples Using Piezoelectric Liquid Dispensing Technology. *NanoWorld J* 1(1): 25-30.

Published by United Scientific Group

Abstract

In the last years, the evolution and the advances of the nanobiotechnologies applied to the systematic study of proteins, namely proteomics, both structural and functional, and specifically the development of more sophisticated and large-scale protein arrays, have enabled scientists to investigate protein interactions and functions with an unforeseeable precision and wealth of details. Here, we present a further advancement of our previously introduced and described Nucleic Acid Programmable Protein Arrays (NAPPA)-based nanoconductometric sensor. We coupled Quartz Crystal Microbalance with Dissipation factor Monitoring (QCM_D) with piezoelectric inkjet printing technology (namely, the newly developed ActivePipette), which enables to significantly reduce the volume of probe required for genes/proteins arrays. We performed a negative control (with master mix, or MM) and a positive control (MM_p53 plus MDM2). We performed this experiment both in static and in flow, computing the apparent dissociation constant of p53-MDM2 complex (130 nM, in excellent agreement with the published literature). We compared the results obtained with the ActivePipette printing and dispensing technology vs. pin spotting. Without the ActivePipette, after MDM2 addition the shift in frequency (Δf) was 7575 Hz and the corresponding adsorbed mass was 32.9 μg. With the ActivePipette technology, after MDM2 addition Δf was 7740 Hz and the corresponding adsorbed mass was 33.6 μg. With this experiment, we confirmed the sensing potential of our device, being able to discriminate each gene and protein as well as their interactions, showing for each one of them a unique conductance curve. Moreover, we obtained a better yield with the ActivePipette technology,

Keywords

Cell-free expression system, MDM2, Nanoconductometric sensor, NanoProbeAssay, Nucleic Acid Programmable Protein Array (NAPPA), p53, Piezoelectric inkjet printing, Quartz Crystal Microbalance with Dissipation factor Monitoring (QCM_D)

Introduction

In the last decades, the rapidly increasing evolution and the advances of the nanobiotechnologies applied to the systematic study of proteins, namely proteomics, both structural and functional, and specifically the development of more sophisticated and large-scale protein arrays [1], have enabled scientists to investigate protein interactions and functions with an unforeseeable precision and wealth of details [2]. Protein arrays are an important proteomics tool, together with mass spectrometry and 2-dimensional gel electrophoresis [3-6]. Moreover,

so-called cell-free protein arrays [7, 8] can be coupled with label-free approaches: which offer unique advantages in the study of human proteome [9-11].

In this manuscript, we report and discuss some preliminary results of protein expression of genes related to cancer, coupling Nucleic Acid Programmable Protein Array (NAPPA) with a recently improved nanogravimetric apparatus which exploits the quartz crystal microbalance with frequency (QCM_F) and quartz crystal microbalance with dissipation monitoring (QCM_D) technologies [11, 12] and using a newly developed piezoelectric liquid dispensing technology.

The selected proteins are p53 and MDM2 because of their importance and biological roles, which will be briefly summarized and reviewed in the following paragraphs.

p53, as a nuclear transcription factor and oncosuppressor, plays a major role in the regulation of the cell cycle, DNA repair, and cell death/senescence/apoptosis, responding to DNA damage, hypoxia, oncogene activation and other kinds of stress. It finely tunes survival of proteins in the mitochondria, microRNA processing, and protein translation among the other biological processes in which it is involved [13]. Mouse double minute 2 homolog protein (MDM2) is one of the main p53 negative regulators since it acts as an E3 ubiquitin ligase that catalyzes the ubiquitination of p53 for degradation, recognizing the N-terminal trans-activation domain (TAD) of p53 [14]. Inhibitors that target p53, MDM2 or p53/MDM2 interaction are an important class of anticancer therapeutics [14, 15].

At a molecular level, MDM2 has a deep binding pocket for p53, which is only 18 Å long but is fundamental for the interaction with p53's Trp23, Leu26, and Phe19 (the so-called "three finger pharmacophore" model) [13].

We chose NAPPA since this innovative technology avoids any time-consuming task in the difficult process of obtaining highly purified proteins, relying instead on the production of proteins from high quality super-coiled DNA. For this purpose, complementary DNAs (cDNAs) of selected genes tagged with a C-terminal glutathione S-transferase (GST) are spotted on the microarray surface and expressed using a cell-free transcription/translation system (IVTT, in vitro transcription and translation). The newly expressed protein is captured on the array by an anti-GST antibody that have been co-immobilized with the expression clone on the microarray surface.

The advantages and benefits of NAPPA technologies can be briefly summarized [11]:

(1) The demanding and challenging process of obtaining highly purified proteins is replaced by a single quick step; furthermore, cDNAs and clones are more easily available;

(2) Proteins expressed on the NAPPA arrays are stable, properly folded and biologically, functionally active.

NAPPA microarrays can be useful in biomarkers discovery and for other clinical applications [16], such as biosensor development, especially in the effort of moving towards Personalized Medicine [17-19]. For this task we coupled NAPPA with a new generation of conductometric devices, namely QCM. QCM_D indeed appears a promising tool to study protein-protein interactions especially in the field of oncology, both cellular and molecular.

Inkjet printing confers more advantages: in the field of nanotechnologies, it has been exploited to produce a formulation capable of controlling the release of a drug [20], to better functionalize biosensors [21-24].

To the best of our knowledge, we coupled for the first time QCM_D with NAPPA technology and piezoelectric inkjet printing for biomedical applications. The objective of the present research regards the analysis of protein-protein interaction towards potentially useful clinical applications, namely in the field of cancer studies.

Clinical implications are also envisaged and addressed.

Materials and Methods

QCM_D conductometer

Nanogravimetry makes use of functionalized piezoelectric quartz crystals (QC), which vary their resonance frequency (f) when a mass (m) is adsorbed to or desorbed from their surface. This is well described by the well-known Sauerbrey's equation:

$$\Delta f = S \cdot \Delta m = -2 \cdot f^2/Z_p \cdot \Delta m$$

where Δf is the frequency shift, Δm is the change of mass per area, S is the mass sensitivity, f is the resonant frequency, Z_p is the acoustical impedance.

This equation can be expressed also as:

$$\Delta f/f_0 = - m/(A \cdot \rho \cdot l)$$

where f_0 is the fundamental frequency, A is the surface area covered by the adsorbed molecule and ρ and l are the quartz density and thickness, respectively.

Quartz resonators response strictly depends on the biophysical properties of the analyte, such as the viscoelastic coefficient. The dissipation factor (D) of the crystal's oscillation is correlated with the softness of the studied material and its measurement can be computed by taking into account the bandwidth of the conductance curve 2Γ, according to the following equation:

$$D = 2\Gamma/f$$

where f is the peak frequency value.

In our analysis we introduced also a "normalized D factor", D_N, that we defined as the ratio between the half-width half-maximum (Γ) and the half value of the maximum value of the conductance (G_{max}) of the measured conductance curves [11]:

$$D_N = 2\Gamma/G_{max}$$

D_N is more strictly related to the curve shape, reflecting the conductance variation [2, 11].

ActivePipette piezoelectric inkjet technology

For this experiment, we exploited a newly developed technology that enables to significantly reduce the volume of probe required for genes/proteins arrays [25-27]. This technology relies upon the precise, non-contact printing capabilities of a piezoelectric inkjet printer. When compared to

pin spotters, it enables to avoid some drawbacks, such as slow printing and dispensing speed, satellite spots, ring-like stains or "coffee mug" effects, inhomogeneous spots, misplaced or even absent spots due to evaporation issues and poorly controlled deposition and confinement, and spot contamination [27, 28]. Moreover, two important advantages of piezoelectric inkjet printing are the possibility of spotting on complex surfaces [27, 29] and using also clinical samples of limited volume and amount, thus showing more biotechnological and biomedical potential and implications.

NAPPA experiments

The QCM_D instrument was developed by Elbatech (Elbatech srl, Marciana – LI, Italy). The quartz was connected to an RF gain-phase detector (Analog Devices, Inc., Norwood, MA, USA) and was driven by a precision DDS (Analog Devices, Inc., Norwood, MA, USA) around its resonance frequency, thus acquiring a conductance versus frequency curve ("conductance curve") which shows a typical Gaussian behavior. The conductance curve peak was at the actual resonance frequency while the shape of the curve indicated how the viscoelastic effects of the surrounding layers affected the oscillation. The QCM_D software, QCMAgic-Q5.3.256 (Elbatech srl, Marciana – LI, Italy) allows to acquire the conductance curve or the frequency and dissipation factor variation versus time. In order to have a stable control of the temperature, the experiments were conducted in a temperature chamber. Microarrays were produced on standard nanogravimetry quartz used as highly sensitive transducers. The QC expressing proteins consisted of 9.5 MHz, AT-cut quartz crystal of 14 mm blank diameter and 7.5 mm electrode diameter, produced by ICM (Oklahoma City, USA). The electrode material was 100Å Cr and 1000Å Au and the quartz was embedded into glass-like structures for easy handling [11, 30].

The NAPPA-QC arrays were printed with 100 spots per QC.

Quartzes gold surfaces were coated with cysteamine to allow the immobilization of the NAPPA printing mix. Briefly, quartzes were washed three times with ethanol, dried with Argon and incubated over night at 4°C with 2 mM cysteamine. Quartzes were then washed three times with ethanol to remove any unbound cysteamine and dried with Argon. Plasmids DNA coding for GST tagged proteins were transformed into *E. coli* and DNA were purified using the NucleoPrepII anion exchange resin (Macherey Nagel). NAPPA printing mix was prepared with 1.4 µg/ul DNA, 3.75 µg/ul BSA (Sigma-Aldrich), 5mM BS3 (Pierce, Rockford, IL, USA) and 66.5 µg polyclonal capture GST antibody (GE Healthcares). Negative controls, named master mix (hereinafter abbreviated as "MM"), were obtained replacing DNA for water in the printing mix. Samples were incubated at room temperature for 1 hour with agitation and then printed on the cysteamine-coated gold quartz using the Qarray II from Genetix. In order to enhance the sensitivity, each quartz was printed with 100 identical features of 300 microns diameter each, spaced by 350 microns center-to-center. The human cDNAs immobilized on the NAPPA-QC were: p53 and MDM2.

Gene expression was performed immediately before the assay, following the protocol described in [11]. Briefly,

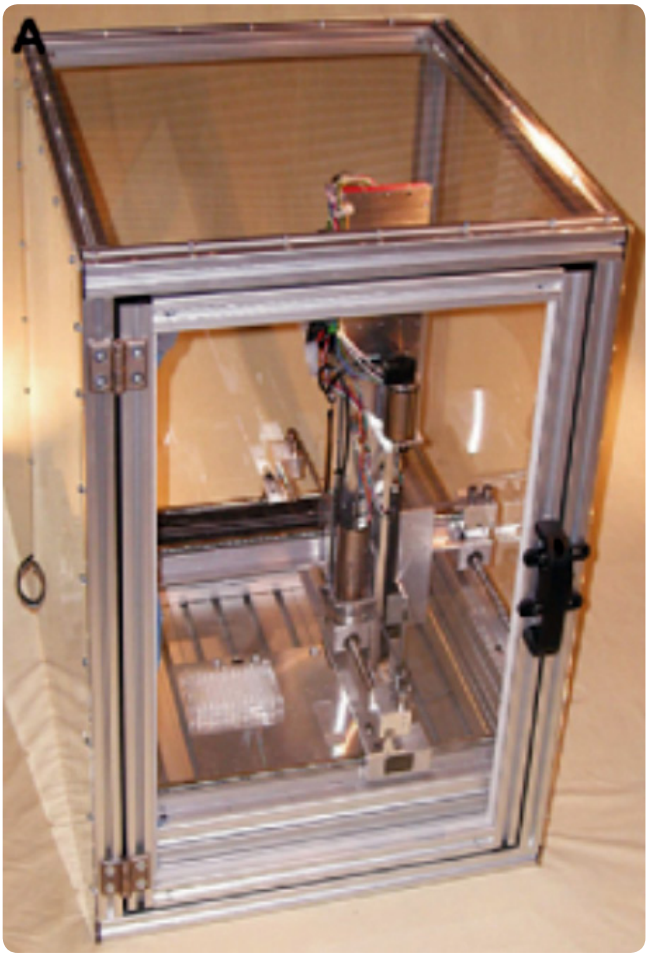

Figure A: Piezoelectric liquid dispensing for printing and probing of NanoProbeArrays.

IVTT was performed using HeLa lysate mix (1-Step Human Coupled IVTT Kit, Thermo Fisher Scientific Inc.), prepared according to the manufacturers' instructions. The quartz, connected to the nanogravimeter inside the incubator, was incubated for 10 min at 30°C with 40 µl of HeLa lysate mix for proteins synthesis and then, the temperature was decreased to 15°C for a period of 5 min to facilitate the proteins binding on the capture antibody (anti-GST). After the protein expression and capture, the quartz was removed from the instrument and washed at room temperature, in 500 mM NaCl PBS for 3 times. The protocol described above was followed identically for both negative control QC (the one with only MM, i.e, all the NAPPA chemistry except the cDNA) and protein displaying QC.

After protein expression, capture, and washing the QCs were used for the interaction studies QC displaying the expressed protein was spotted with 40 µl of MDM2 at 22°C.

Reproducibility of the experiments was assessed computing the coefficient of variation (CV, or σ^*), using the following equation:

$$\sigma^* = \sigma/\mu,$$

where σ is the standard deviation, and μ is the mean.

We performed experiment both in static and in flow. This method enables to compute the apparent dissociation constant, using the following equation [31]:

where $f(t)$ is the frequency at time t, t_0 represents the start of dissociation, f_0 is the frequency at t_0, k_{diss} is the apparent dissociation rate constant.

Results and Discussion

QCM_D measures were calibrated for frequency and for D factor shifts. The calibration curves equation (obtained with Ordinary Least Squares methods, OLS) are:

$\Delta f = -7.16 - 231.18\ m$; with $r^2 = 0.9986$,

and:

$D = 0.831 + 0.286\ \eta$; with $r^2 = 0.9990$.

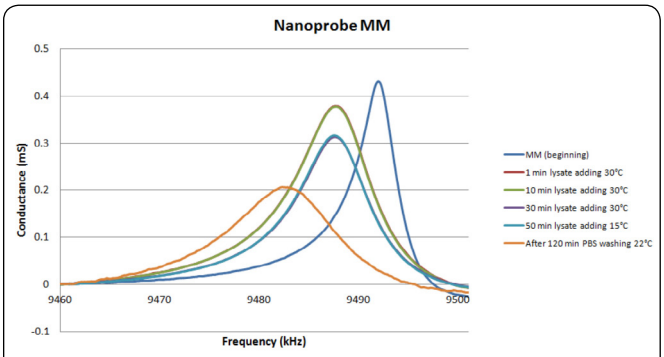

Figure 1: Conductance curves of MM QC (upper). The curves were collected in different steps of NAPPA protocol, as reported in the legend.

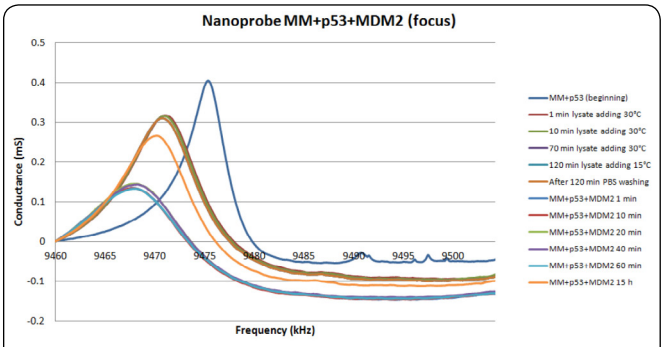

Figure 2: Conductance curves of MM_p53 QC. The curves were collected in different steps of NAPPA protocol, as reported in the legend, and after MDM2 addition.

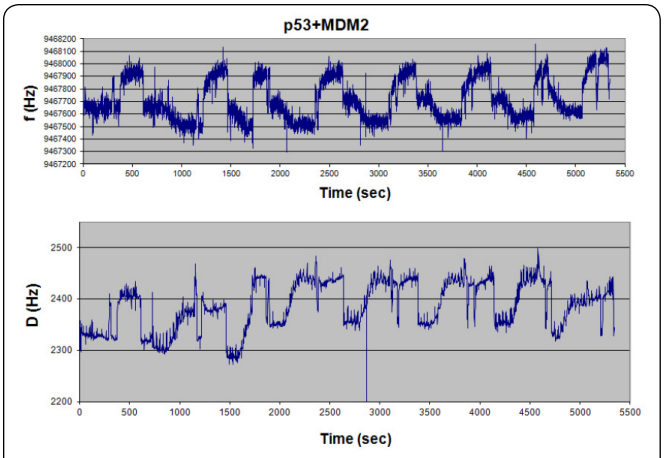

Figure 3: Flow interaction between p53 and MDM2 in solution.

We analyzed the conductance curves acquired in NAPPA-QCs in different steps of the expressing and capturing process: after the addition of human IVTT lysate at 30°C ("IVTT addition"), *i.e.* prior protein expression; after the final washing process with PBS ("Post-wash"); after addition of the substrate.

In Figure 1 are reported the conductance curves of the negative control (MM experiment), while in Figure 2 are shown the conductance curves of quartz carrying p53 gene being expressed and thereafter interacting with MDM2 are reported.

Figure 3 shows the same experiment of Figure 2 conducted in flow (frequency *versus* time, and D factor *versus* time).

We computed the apparent dissociation constant of the p53-MDM2 complex 130 nM, which is in excellent agreement with the extant literature [32].

Conductance curves	f(Hz)b	Γ(Hz)b	Gmax (mS)b	D X 103 c	DN(Hz/mS)c
MM					
Beginning	9491920	5610	0,43	0,59	13001,16
IVTT addition 1 min 30°C	9487615	10020	0,38	1,056	26382,31
IVTT addition 10 min 30°C	9487615	10020	0,38	1,056	26458,94
IVTT addition 30 min 30°C	9487510	9270	0,31	0,98	29626,08
IVTT addition 50 min 15°C	9487450	7710	0,32	0,81	24329,44
After 120 min post PBS washing 22°C	9482245	12150	0,21	1,28	58923,38

[a]Conductance curves were collected in different steps of NAPPA protocol. [b]f is peak frequency, Γ is the half-width half-maximum (HWHM), and G_{max} is the maximum conductance. [c]D factor and D_N (computed as $D_N = 2\Gamma/G_{max}$) normalized D factor.

Table 1: Main Parameters of QC-NAPPA Displaying MM (as a negative control)[a].

Conductance curves	CV (%)a	ΔDb	ΔDN (Hz/mS)b	Δf (Hz)c	Δf (Hz)c	m (µg)c	m' (µg)c
MM							
IVTT addition 1 min 30°C	3,2	-	-	-4305	-	18,7	-
IVTT addition 10 min 30°C	3,8	0	76,6	-4305	0	18,7	0
IVTT addition 30 min 30°C	4,5	-0,08	3243,8	-4410	105	19,1	0,5
IVTT addition 50 min 15°C	3,1	-0,24	-2052,9	-4470	165	19,4	0,7

[a]Coefficient of variation of three independent experiments. [b]D factor and normalized D factor shifts (ΔD and ΔD_N) respect the values immediately after lysate addition [c]Frequency shifts respect the initial frequency (Δf) and respect the frequency immediately after lysate addition (Δf') and corresponding molecular masses (m and m').

Table 2: Shift of the Main Parameters of MM and p53 Conductance Curves after Lysate Addition and MDM2 addition, and the Corresponding Mass of Immobilized Protein on the QC Surface.

In Tables 1-4, the main parameters of the conductance curves of Figure 1 and 2 are reported.

In Table 5, we compared the results obtained with the piezoelectric inkjet printing and dispensing ActivePipette technology with the values yielded without [30]. We can see that without the ActivePipette, after expressing the protein and washing Δf was 4530 Hz and the corresponding adsorbed mass was 19,7 µg, while after MDM2 addition Δf was 7575 Hz and the corresponding adsorbed mass was 32,9 µg.

With the ActivePipette technology, after expressing the protein and washing Δf was 4665 Hz and the corresponding adsorbed mass was 20,3 μg, while after MDM2 addition Δf was 7740 Hz and the corresponding adsorbed mass was 33.6 μg.

Conductance curves	f(Hz)[b]	Γ(Hz)[b]	G_{max} (mS)[b]	D X 10^3 [c]	D_N (Hz/mS)[c]
MM_p53					
Beginning	9475375	5190	0,41	0,55	12795,86
IVTT addition 1 min 30°C	9471055	8040	0,32	0,85	25267,13
IVTT addition 10 min 30°C	9470950	8010	0,32	0,85	25348,1
IVTT addition 70 min 30°C	9470710	7950	0,31	0,84	25546,27
IVTT addition 120 min 15°C	9470710	7950	0,31	0,84	25546,27
After 120 min post PBS washing	9470710	7950	0,31	0,84	25546,27
MM_p53 plus MDM2					
1 min	9467770	8460	0,14	0,89	62527,72
10 min	9467635	8220	0,14	0,87	60798,82
20 min	9467875	7140	0,15	0,75	49139,71
40 min	9468175	6570	0,14	0,69	45720,25
60 min	9468100	9000	0,13	0,95	67164,18
15 h	9470170	8190	0,27	0,86	30639,73

[a]Conductance curves were collected in different steps of NAPPA protocol. [b]f is peak frequency, Γ is the half-width half-maximum (HWHM), and G_{max} is the maximum conductance. [c]D factor and D_N (computed as $D_N = 2\Gamma/G_{max}$) normalized D factor.

Table 3: Main Parameters of QC-NAPPA Displaying MM_p53 plus MDM2 (focus experiment)[a].

Conductance curves	C_V (%)[a]	ΔD[b]	ΔD_N (Hz/mS)[b]	Δf (Hz)[c]	Δf (Hz)[c]	m (μg)[c]	m' (μg)[c]
MM_p53							
IVTT addition 1 min 30°C	3,2	-	-	-4320	-	18,8	-
IVTT addition 10 min 30°C	4,2	-0,003	81	-4425	105	19,2	0,5
IVTT addition 70 min 30°C	3,5	-0,01	279	-4665	345	20,3	1,5
IVTT addition 120 min 15°C	4,1	-0,01	279	-4665	345	20,3	1,5
MM_p53 plus MDM2							
1 min	3,8	0,04	37260,6	-7605	3285	33	14,3
10 min	4,1	0,02	35531,7	-7740	3420	33,6	14,9
20 min	3,5	-0,09	23872,6	-7500	3180	32,6	13,8
40 min	3,7	-0,16	20453	-7200	2880	31,3	12,5
60 min	4,2	0,1	41897	-7275	2955	31,6	12,8
15 h	4,1	0,02	5372,6	-5205	885	22,6	3,8

[a]Coefficient of variation of three independent experiments. [b]D factor and normalized D factor shifts (ΔD and ΔD_N) respect the values immediately after lysate addition [c]Frequency shifts respect the initial frequency (Δf) and respect the frequency immediately after lysate addition (Δf') and corresponding molecular masses (m and m').

Table 4: Shift of the Main Parameters of MM and p53 Conductance Curves after Lysate Addition and MDM2 addition, and the Corresponding Mass of Immobilized Protein on the QC Surface.

Conductance curves	f(Hz)[a]	f(Hz)[b]	Γ (Hz)[a]	Γ (Hz)[b]	G_{max} (mS)[a]	G_{max} (mS)[b]	D_N (Hz/mS)[a]	D_N (Hz/mS)[b]
Beginning	9475435	9475375	2220	5190	0,42	0,41	10699	12796
After protein expression and washing	9470905	9470710	3705	7950	0,31	0,31	23903	25546
After MDM2 addition	9467860	9467635	3600	8220	0,14	0,14	53333	60799

Table 5: Comparison between the MM_p53 plus MDM2 experiment carried out with the traditional technology (a) (published in Nicolini et al., 2012) and experiment with the ActivePipette piezoelectric inkjet dispensing technology (b).

Conclusions

In this paper, we successfully introduced an advancement in our previously described NAPPA-based nanoconductometric sensor, coupling it with a newly developed piezoelectric inkjet printing and dispensing technology (namely, the ActivePipette). We performed a negative control (MM) and a positive control (MM_p53 plus MDM2). We confirmed the sensing potential of our device, being able to discriminate each gene and protein as well as their interactions, showing for each one of them a unique conductance curve. Moreover, in this communication, we showed that we obtained a better yield with ActivePipette piezoelectric dispensing technology.

Acknowledgements

This project was supported by grants to FEN (Fondazione Elba Nicolini) and to Professor Claudio Nicolini of the University of Genova, Italy by the FIRB Nanobiosensors (ITALNANONET RBPR05JH2P_003) and by a grant Funzionamento from MIUR (Ministero dell'Istruzione, Università e Ricerca; Italian Ministry for Research and University). The authors are very grateful to Prof. Joshua LaBaer for his precious cooperation at the Virginia G. Piper Center for Personalized Diagnostics, Biodesign Institute, Arizona State University, Tempe, AZ. USA during Professor Nicolini Visting Professorship stage. ActivePipette piezoelectric inkjet dispensing technology was provided by Engineering Arts (Tempe, AZ).

References

1. Pratsch K, Wellhausen R, Seitz H. 2014. Advances in the quantification of protein microarrays. *Curr Opin Chem Biol* 18: 16-20. doi:10.1016/j.cbpa.2013.10.024
2. Bragazzi NL, Spera R, Pechkova E, Nicolini C. 2014. NAPPA-based nanobiosensors for the detection of proteins and of protein-protein interactions relevant to cancer. *J Carcinog & Mutagen* 5: 166. doi: 10.4172/2157-2518.1000166
3. Aldred S, Grant MM, Griffiths HR. 2004. The use of proteomics for the assessment of clinical samples in research. *Clin Biochem* 37(11): 943-952. doi:10.1016/j.clinbiochem.2004.09.002
4. Baggerman G, Vierstraete E, De Loof A, Schoofs L. 2005. Gel-based versus gel-free proteomics: a review. *Comb Chem High Throughput Screen* 8(8): 669-677. doi: 10.2174/138620705774962490
5. Forler S, Klein O, Klose J. Individualized proteomics. 2014. *J Proteomics* 107 :56-61. doi:10.1016/j.jprot.2014.04.003

6. Rodrigo MA, Zitka O, Krizkova S, Moulick A, Adam V, et al. 2014. MALDI-TOF MS as evolving cancer diagnostic tool: a review. *J Pharm Biomed Anal* 95: 245-255. doi:10.1016/j.jpba.2014.03.007
7. Ramachandran N, Hainsworth E, Bhullar B, Eisenstein S, Rosen B, et al. 2004. Self-assembling protein microarrays. *Science* 305(5680): 86-90. doi:10.1126/science.1097639
8. Ramachandran N, Raphael JV, Hainsworth E, Demirkan G, Fuentes MG, et al. 2008. Next-generation high-density self-assembling functional protein arrays. *Nat Methods* 5(6): 535-538. doi:10.1038/nmeth.1210
9. Bragazzi NL, Pechkova E, Nicolini C. 2014. Proteomics and proteogenomics approaches for oral diseases. *Adv Protein Chem Struct Biol* 95: 125-162. doi:10.1016/B978-0-12-800453-1.00004-X
10. Hunter AC. 2009. Application of the quartz crystal microbalance to nanomedicine. *J Biomed Nanotechnol* 5(6): 669-675. doi: 10.1166/jbn.2009.1083
11. Spera R, Festa F, Bragazzi NL, Pechkova E, LaBaer J, et al. 2013. Conductometric monitoring of protein-protein interactions. *J Proteome Res* 12(12): 5535-5547. doi: 10.1021/pr400445v
12. Nicolini C, Bragazzi N, Pechkova E. 2012. Nanoproteomics enabling personalized nanomedicine. *Adv Drug Deliv Rev* 64(13): 1522-1531. doi:10.1016/j.addr.2012.06.015
13. Khoury K, Dömling A. 2012. P53 mdm2 inhibitors. *Curr Pharm Des* 18(30): 4668-4678. doi: 10.2174/138161212802651580
14. Pei D, Zhang Y, Zheng J. 2012. Regulation of p53: a collaboration between Mdm2 and Mdmx. *Oncotarget* 3(3): 228-235.
15. Wang W, Hu Y. 2012. Small molecule agents targeting the p53-MDM2 pathway for cancer therapy. *Med Res Rev* 32(6): 1159-1196. doi: 10.1002/med.20236
16. Casado-Vela J, Fuentes M, Franco-Zorrilla JM. 2014. Screening of protein-protein and protein-dna interactions using microarrays: applications in biomedicine. *Adv Protein Chem Struct Biol* 95: 231-281. doi: 10.1016/B978-0-12-800453-1.00008-7
17. He M, Stoevesandt O, Taussig MJ. 2008. In situ synthesis of protein arrays. *Curr Opin Biotechnol* 19(1): 4-9. doi: 10.1016/j.copbio.2007.11.009
18. Nand A, Gautam A, Pérez JB, Merino A, Zhu J. 2012. Emerging technology of in situ cell free expression protein microarrays. *Protein Cell* 3(2): 84-88. doi: 10.1007/s13238-012-2012-y
19. Takulapalli BR, Qiu J, Magee DM, Kahn P, Brunner A, et al. 2012. High density diffusion-free nanowell arrays. *J Proteome Res* 11(8): 4382-4391. doi: 10.1021/pr300467q
20. Scoutaris N, Alexander MR, Gellert PR, Roberts CJ. 2011. Inkjet printing as a novel medicine formulation technique. *J Control Release* 156(2): 179-185. doi: 10.1016/j.jconrel.2011.07.033
21. Kirk JT, Fridley GE, Chamberlain JW, Christensen ED, Hochberg M, et al. 2011. Multiplexed inkjet functionalization of silicon photonic biosensors. *Lab Chip* 11(7): 1372-1377. doi: 10.1039/c0lc00313a
22. Yun YH, Lee BK, Choi JS, Kim S, Yoo B, et al. 2011. A glucose sensor fabricated by piezoelectric inkjet printing of conducting polymers and bienzymes. *Anal Sci* 27(4): 375. doi: 10.2116/analsci.27.375
23. Fujita S, Onuki-Nagasaki R, Fukuda J, Enomoto J, Yamaguchi S, et al. 2013. Development of super-dense transfected cell microarrays generated by piezoelectric inkjet printing. *Lab Chip* 13(1): 77-80. doi: 10.1039/c2lc40709d
24. Yamaguchi S, Ueno A, Akiyama Y, Morishima K. 2012. Cell patterning through inkjet printing of one cell per droplet. *Biofabrication* 4(4): 045005. doi: 10.1088/1758-5082/4/4/045005
25. Nagaraj VJ, Eaton S, Thirstrup D, Wiktor P. 2008. Piezoelectric printing and probing of Lectin NanoProbeArrays for glycosylation analysis. *Biochem Biophys Res Commun* 375(4): 526-530. doi: 10.1016/j.bbrc.2008.08.033
26. Nagaraj VJ, Aithal S, Eaton S, Bothara M, Wiktor P, et al. 2010. NanoMonitor: a miniature electronic biosensor for glycan biomarker detection. *Nanomedicine (Lond)* 5(3): 369-378. doi: 10.2217/nnm.10.11
27. Nagaraj VJ, Eaton S, Wiktor P. 2011. NanoProbeArrays for the analysis of ultra-low-volume protein samples using piezoelectric liquid dispensing technology. *J Lab Autom* 16(2): 126-133. doi: 10.1016/j.jala.2010.07.005
28. Barbulovic-Nad I, Lucente M, Sun Y, Zhang M, Wheeler AR, et al. 2006. Bio-microarray fabrication techniques – a review. *Crit Rev Biotechnol* 26(4): 237-259. doi: 10.1080/07388550600978358
29. Sumerel J, Lewis J, Doraiswamy A, Deravi LF, Sewell SL, et al. 2006. Piezoelectric ink jet processing of materials for medical and biological applications. *Biotechnol J* 1(9): 976-987. doi: 10.1002/biot.200600123
30. Nicolini C, Adami M, Sartore M, Bragazzi NL, Bavastrello V, et al. 2012. Prototypes of newly conceived inorganic and biological sensors for health and environmental applications. *Sensors (Basel)* 12(12): 17112-17127. doi: 10.3390/s121217112
31. Hauck S, Drost S, Prohaska E, Wolf H, Dübel S. 2002. Analysis of Protein Interactions Using Microbalance Biosensor. In Protein-Protein Interactions: A Mol Cloning Manual, Cold Spring Harbor Laboratory Press, pp 273-283.
32. Chène P. 2004. Inhibition of the p53-MDM2 interaction: targeting a protein-protein interface. *Mol Cancer Res* 2(1): 20-28.